Title
The Application of Autocorrelation SETI Search Techniques in an ATA Survey

Journal
The Astrophysical Journal, 869(1)

ISSN
0004-637X

Authors
Harp, GR
Ackermann, RF
Astorga, Alfredo
et al.

Publication Date
2018-12-10

DOI
10.3847/1538-4357/aaeb98

Peer reviewed

A Radio SETI Campaign for μs-s Periodic Signals

Short title: SETI Autocorrelation Survey with ATA

G. R. Harp[1], R. F. Ackermann[1], Alfredo Astorga[1], Jack Arbunich[1], Kristin Hightower[1], Seth Meitzner[1], W. C. Barott[2], Michael C. Nolan[3], D. G. Messerschmitt[4], Douglas A. Vakoch[1], Seth Shostak[1], J. C. Tarter[1]

[1] Center for SETI Research, SETI Institute, 189 Bernardo Ave., Ste. 100, Mountain View, CA, 94043.

[2] Electrical & System Engineering Dept., Embry-Riddle Aeronautical University, 600 S. Clyde Morris Blvd, Daytona Beach, FL, USA, 32114.

[3] Arecibo Observatory, HC3 Box 53995, Arecibo, PR 00612, USA.

[4] Department of Electrical Engineering and Computer Sciences, University of California at Berkeley, 387 Soda Hall, Berkeley, CA 94720-1776.

Abstract
We report a novel radio autocorrelation (AC) search for extraterrestrial intelligence (SETI). For selected frequencies across the terrestrial microwave window (1-10 GHz) observations were conducted at the Allen Telescope Array to identify artificial non-sinusoidal periodic signals with radio bandwidths greater than 1 kHz, which are capable of carrying substantial messages with symbol-rates from 10-10^6 Hz. Out of 243 observations, about half (101) were directed toward sources with known continuum flux > ~1 Jy (quasars, pulsars, supernova remnants and masers), based on the hypothesis that they might harbor heretofore undiscovered natural or artificial, repetitive, phase or frequency modulation. The rest of the targets were mostly toward exoplanet stars and similarly interesting targets from the standpoint of SETI. This campaign rules out several previously untested hypotheses relating to the number of artificially modulated "natural" sources. Since we are using a phase sensitive detector, these observations break new ground on this topic. We conclude that the probability that future observations like the ones described here will reveal repetitively modulated emissions from a wide variety of sources, including quasars, supernova remnants and bright stars, is no more than 15–30 percent, depending on signal type. The paper concludes by describing an approach to expanding this survey to many more targets and much greater sensitivity using archived and real-time data from interferometers all over the world.

Keywords: astrobiology; autocorrelation; instrumentation: detectors; instrumentation: interferometers; SETI; METI

1 Introduction

Searches for Extraterrestrial Intelligence (SETI) at radio frequencies traditionally focus on slowly modulated narrowband signals (Cocconi, G. & Morrison, P. 1959; Drake, F. D. 1961; Oliver, B. M. & Billingham, J. 1971; Tarter, J. C. 2001; Shuch, H. P. 2011). The premise of the narrowband (~1 Hz) search is that relatively weak narrowband ETI signals may be present but hidden in ordinary astronomical observations.

One unspoken assumption is that all radio sources already known to astronomers have a natural origin. This paper recognizes that this statement is not fully supported with existing observations. Some well-known strong radio sources might harbor a hidden message masquerading as, or piggybacking on, a strong natural source. While many pulsars and other sources may have been previously tested for repetitive power modulation, the authors are not aware of previous work testing for encodings that use e.g. constant-power phase modulation from known bright sources. The latter is the focus here.

Suppose ET were to construct a powerful transmitter sending information at a kHz to GHz bit rate. Over the bandwidth of transmission and to most current radio telescopes, such a transmitter is indistinguishable from a natural continuum source because the time fluctuations are too short to appear in standard detectors. However, these same signals can be detectable by autocorrelating the electric field amplitude and phase, otherwise known as an autocorrelation (AC) detection. Here we present what we believe to be the first radio search for ETI using AC detection of complex signals containing an element of repetition.

Recently there has been a resurgence of theoretical research on discovery of *wideband* engineered signals that may be used for interstellar messaging (Harp, G. R. et al. 2010a; Morrison, I. S. 2011a; Siemion, A. et al. 2010; Messerschmitt, D. G. & Morrison, I. S. 2012; Harp, G. R. et al. 2012; Von Korff, J. et al. 2013; Gardner, W. A. & Spooner, C. M. 1992). Meanwhile, techniques developed for very long baseline interferometry have been adapted to capture substantial bandwidths (>1 MHz) of digitized time series data for post-processing (Harp, G. R. et al. 2010a; Siemion, A. et al. 2010; Korpela, B. E. et al. 2001; Tarter, J. C. et al. 2010; Wayth, R. B. et al. 2011; Morrison, I. S. 2012), often using processing that could not be performed in real time. This paper reports SETI observations that make use of such non-traditional approaches.

1.1 Conventional Matched Filter Bank Searches and AC

Narrowband and pulse searches in SETI/astronomy depend upon the assumption of preconceived signal types: narrowband/pulsed signals. Such sources appear as narrow sloping or slightly curved traces in a frequency vs. time waterfall plot (c.f. Figure 1). The intensity-inverted waterfalls of Figure 1 portray a narrowband signal from the ISSE3 spacecraft (left) and a dispersed pulse of radiation from the Crab pulsar (right). To highlight the similarity of the waterfalls, the space and frequency axes are swapped between left and right images. The ISEE3 signal is not vertically aligned because of the relative acceleration between spacecraft and detector. The pulse is similarly slanted for a different reason: Light propagation in the interstellar medium is dispersed (increasingly retarded at lower frequencies).

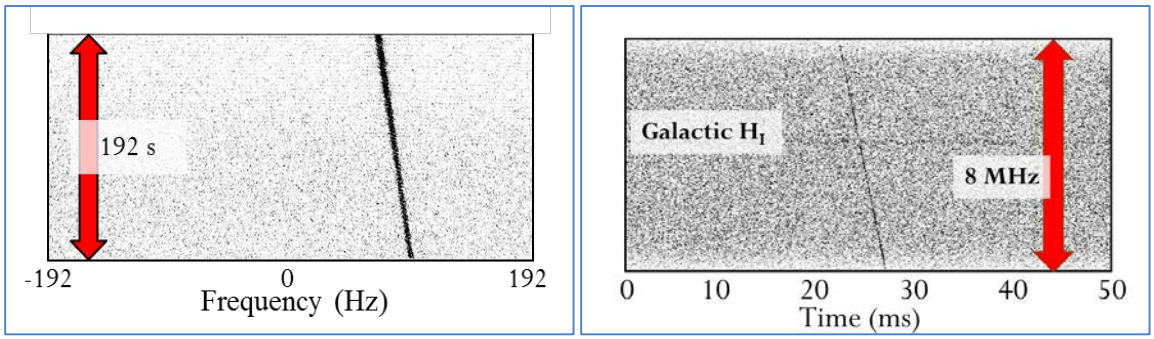

Figure 1: (Left) Time versus frequency waterfalls taken at ATA where the dark trace indicates detection of a narrowband transmission from spacecraft ISEE3 during its closest approach to Earth. (Right) Frequency versus time waterfall where narrow dark trace indicates detection of one wideband "giant pulse" from the Crab pulsar. The horizontal line corresponds to galactic HI at 1420 MHz.

Searches for such signals look for modestly curved traces in the time-frequency domain having small perpendicular cross-section (width << cross-width[1]). Such searches can be

[1] The variables length l and width w require a definition of units to be compared. One way of consistently defining units is to measure l in units of the inverse width w^{-1}. On the left side of Figure 1, $w \sim 5$ Hz implying a time unit of 0.2 s, hence $l \sim 192 / 0.2 = 960$ time units perpendicular to w. On the right side, $w \sim 0.2$ s implies a frequency unit of 5, and $l = 8 \times 10^6 / 5 = 2 \times 10^5$. In both cases, $w << l$ is satisfied, which is the working definition of a "trace" in a waterfall.

parameterized with 2 to 3 independent parameters: the frequency f, drift rate df/dt, and sometimes $d^2 f / dt^2$. In pulse searches, the parameters are swapped: t, dt / df, $d^2 t / df^2$.

Signals are detected using a matched filter bank (MFB) which effectively prepares a set of test waveforms spanning the parameter ranges and compares them to the observed waveform. With current technology, the MFBs are compute bound; computation time for an MFB do not scale well, increasing geometrically with the number of parameters. For this reason, modern searches place severe restrictions on the ranges of search coefficients for first and second derivatives, and additional parameters are out of the question. The benefit of MFBs is their sensitivity. Historically it has been argued that it is better to search a narrow signal space with greatest sensitivity than to search widely with moderate sensitivity (Oliver, B. M. & Billingham, J. 1971).

In this campaign, we use AC detection rather than an MFB. The search philosophy here is that we wish to maximize the product of two factors:

1. A factor N_{Types} that measures the number of signal types probed in a given search.
2. A factor N_{Stars} which measures the number of stars from which signal detection is possible given a fixed ET transmitter power and ATA's detection sensitivity for that search.

We shall see below that AC detection of artificial signals is less sensitive (requires stronger transmitters) for detection of new sources than total power or MFB detection. Yet the number of signal types probed is astronomically larger, tilting the figure of merit $N_{\text{Stars}} N_{\text{Types}}$ strongly in favor of AC over MFB when computation resources are limited.[2] We shall argue that it makes sense to implement all of total power, narrowband and AC detectors for future SETI observations, especially when using radio interferometers.

1.2 Research Hypotheses

To summarize, this observational campaign tests the following hypotheses (with more detail to be found in the discussion section):

Hypothesis 1. The emitted electric fields of most previously discovered strong radio sources with flux >1 Jy are modulated with a repeating pattern either directly by extraterrestrials or due to some heretofore unknown physics.

Hypothesis 2. Most bright pulsars, besides their characteristic repetitive nature, are additionally modulated as above.

Hypothesis 3. Most confirmed or "candidate" exoplanets harbor civilizations that transmit powerful messages using radio frequency beams of modulated electromagnetic radiation.

Hypothesis 4. Out of all the stars in the galaxy, most harbor transmitters, as in 3.

[2] Other figures of merit may result in different conclusions.

We emphasize that to the best of our knowledge these hypotheses cannot be excluded from past observations. This is the first substantial AC ETI search for phase or frequency modulated repetitive signals. We augment this search 3 other detectors, power spectrum, power spectrum of power, and autocorrelation of power as described in Section 2.

Besides the source types mention above, this campaign includes a small number of targets with special interest for SETI such as the galactic anti-center and the Earth-Sun Lagrange L4 point, and many reference observations used as comparators for testing the direction of origin of newly detected candidate signals.

The rest of this paper contains a description of the ETI signal detection techniques used here along with sensitivity calculations and comparisons to traditional matched filtering. Within this discussion we introduce the details of the observations, followed by a few examples of observed spectra. A discussion section summarizes the results and analyzes their meaning. This is followed by a brief demonstration of how repetitive signals can be detected in typical radio interferometer images and how this research can be extended to analysis of large libraries of archived radio interferometer data.

2 Signal Detection Algorithms

Autocorrelation-based detection strategies that have certain advantages over traditional SETI, including 1) fewer assumptions about signal waveform, 2) potential for detecting signals containing messages with substantial information rates, 3) sensitivity to a vast number of signal types, and 4) insensitivity to dispersion in the interstellar medium (Harp, G. R. et al. 2010a) which is critical since wideband signals are dispersed in the interstellar medium.

We demonstrate this immunity to dispersion with a simulation. We model a distant transmitter emitting four narrow pulses centered around 1 GHz and emitted over a period of 4000 seconds as in Figure 2 left (solid line). After traveling 1600 light years through a plasma with mean electron density equal to that of the interstellar medium (0.01 e^- cm^{-3}), the dispersion measure (DM) of the signals will be about 5 pc cm^{-3}. From the well-known formula for cold plasma dispersion, $\text{delay (s)} = 0.00415\, DM / f^2(\text{GHz})$, we calculate the frequency dependent delay of the transmitted pulses Figure 2, left (dots). On the right hand side of Figure 2, we display the complex valued autocorrelation (AC, algorithm defined below) of the received signal with itself (line) compared to an autocorrelation of the signal power (ACP, defined below) which would be appropriate if the pulses from an incoherent transmitter. As expected, the AC detector shows 6 spikes for these 4 pulses (zero delay spike has been suppressed).

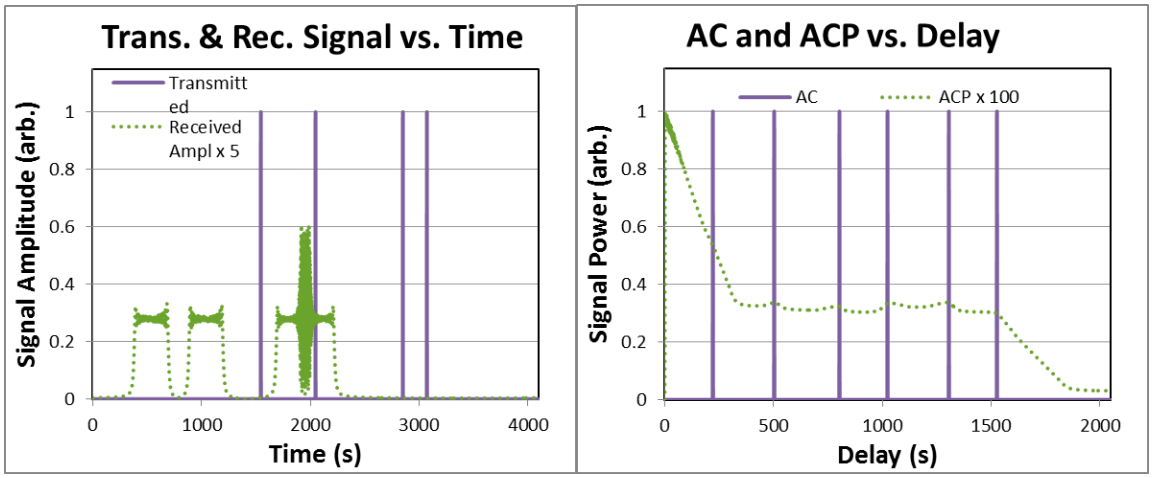

Figure 2: Transmission and reception of a pulsed signal after passage through the interstellar medium far enough to accumulate a dispersion measure of 5 pc cm-3. The left graph compares a baseband copy of the transmitted electric field amplitude at the transmitter (solid line) and receiver (dots). On the right we plot the autocorrelation of the received electric field (AC, line) and autocorrelation of received power (ACP, dots) for the signal. The correlation at zero delay has been suppressed. The detectability of this repetitive signal is much higher for AC. Both methods are used in this paper.

The example of Figure 2 visualizes a more general result: a repetitive signal passed through any stationary linear filter is detected just the same as the unfiltered signal in an AC detector. This means that AC is also immune not only to dispersion but also to the effects of time-invariant scintillation in the interstellar medium.

For coherent signals like in this example, AC discrimination (height of peaks compared to surrounding values) is generally better than for ACP. For constant-power phase or frequency modulated signals, ACP may have zero sensitivity while AC is very sensitive. The known emission processes for natural sources such as pulsars and quasars do not give rise to phase coherent signals and previous studies have focused on power detection methods such as ACP. For this reason, previous studies might have missed constant power phase or frequency modulation (presumably generate by technology) in these emissions and this is what makes the present research novel. The application of AC here is targeting artificial signals.

2.1 Signal Types

The prototype for autocorrelation (AC) detection is a signal having properties that vary statistically with time. AC detection picks up on this time variation even when the modulated signal is otherwise arbitrary. We consider several archetypes for ET signals:

(A) *Narrowband*: We assume a nearly-sinusoidal signal where the coherence time is of order 100 ms or longer. In the workhorse implementation at the ATA, called SonATA, such signals may carry up to 10 bits/s of information. Sometimes we refer to this method as “conventional SETI.”

(B) *Wideband power detection*: With an interferometer like the ATA, it is straightforward to capture frames with many square degree fields of view over time periods from hours to seconds at the ATA. Such power intensity images may be examined for point sources that could be associated with ET transmitters or other unexpected radiation.

(C) *Cyclostationary*: A finite alphabet of radio waveforms representing symbols are transmitted resulting in repetitions at specific delays when the same symbol is transmitted twice. This mode is often used in satellite communication implementing error correction (Morrison, I. S. 2011a; Gardner, W. A. & Spooner, C. M. 1992; Leshem, A. et al. 2000; Morrison, I. S. 2011b). Message information might be encoded in the transmission center frequency, time delay or signal phase. Due to dispersion, the symbols will generally overlap in time. This has little impact on signal detectability unless the delay period is longer than the inverse Doppler drift rate $\left(df\ /\ dt\right)^{-1}$.

With phase modulation, an alphabet may be constructed from a single symbol multiplied by an overall phase factor. Such alphabets correlate after every symbol delay (see e.g. GPS example in (Harp, G. R. et al. 2010a)). An alphabet with non-correlating symbols dilutes the sensitivity of AC detection, but does not substantially alter the conclusions of this paper.

(D) *Amplitude Modulation (AM)*:

a) *Direct transmission.* As with consumer radio, AM is more prone to errors caused by noise and fading than frequency or phase modulation
b) *Receive, delay and transmit (RDT)*: Another suggestion is for ET to set up a transmitter on a line of sight between Earth and a strong radio source such as a quasar. ET collects the quasar signal, amplifies it, and re-transmits a delayed copy toward Earth. Information may be embedded using a time dependent delay.
c) *Source modulation*: Direct amplitude modulation of an astronomical source might be accomplished by modulating or pumping the source itself. As proof of principle, (Weisberg, J. M. et al. 2005) has identified a maser source that is pumped by a pulsar. If we specify the direct modulation in terms of the absolute power of the modulated part of the signal, the sensitivity of an AC search for source modulation is equal to the sensitivity for RTD or direct transmission.

2.2 Sensitivity of Various Detectors

We consider a system where the telescope voltages are digitally sampled and a total of N_s samples are gathered in the observation. For a given threshold X, the total power P_t for an X σ detection of a signal is proportional to the telescope's system equivalent flux density (SEFD), that is, when the astronomical flux density is equal to the system noise power. More precisely,

$$P_t = X\frac{\left(\text{SEFD}\right)}{\sqrt{N_s}}, \qquad \text{where} \qquad \text{SEFD} = \frac{2\eta k_B}{\eta_{eff} A} T_{sys}\ , \tag{1}$$

and $\eta < 1$ is the power loss factor associated with digitization, k_B is Boltzmann's constant, A is the total collecting area and $\eta_{eff} < 1$ is aperture efficiency, or the fraction of A that is captured by the receiver in the combined optical system. At the ATA, $\eta_{eff} = 0.6$ (Harp, G. R. et al. 2011).

During the observation epoch (Jan. 2010 – Mar. 2011) the typical ATA configuration used 25 of the 6.2 m antennas in a phased array beam on the source of interest. The ATA phased array beam diameter is inversely proportional to frequency in GHz with $\theta_{beam} \cong 0.10 / f_{GHz}$. We accumulated 8-bit quadrature digitized data (hence $\eta \approx 1$) with 7 MHz effective bandwidth for typically 10 minutes for an effective total of $N_{samp} = 4.2 \times 10^9$ per observation.

Using measured antenna system temperatures, Table 1 displays the computed sensitivity measures for the various detection algorithms. At four frequencies used in observations, the measured ATA system temperature[3] is used to compute the SNR for a 10 minute observation of a 1 Jy source (e.g. ETI transmitter or a quasar) emitting uniformly over the 7 MHz detector bandwidth in column 3. The 4th column shows the flux of a source detectable at 1σ for a total-power measurement of a wideband signal. For a narrowband (<1 Hz) signal, column 5 shows the minimum detectable flux. Using AC, ACP and PSP detectors, column 6 applies.

Table 1:

Detection Thresholds for Various Algorithms

f (GHz)	Tsys (K)	SNR 1 Jy Source	1σ Wideband Detectable Flux (Jy)	1σ Narrowband Detectable Flux (Jy)	1σ AC, ACP, PSP Detectable Flux (Jy)
1.43	80	129	0.008	504	0.9
3.04	120	86	0.012	756	1.3
6.667	95	108	0.009	598	1.1
8.4	137	75	0.013	863	1.5

The 4th column in Table 1 shows the power detection threshold for a signal whose bandwidth $\mathrm{BW}_{\mathrm{signal}} \geq \mathrm{BW}_{\mathrm{detector}}$. The analogous detection threshold for a narrowband signal is larger by a factor of $\sqrt{N_{chan}}$,[4] where N_{chan} is the number of channels across the detector bandwidth. This is because all the power in the threshold wideband signal must be reproduced in a single channel. The detection thresholds for a 1 Hz bandwidth signal

[3] New receivers are presently being installed at ATA which have lower system temperatures are currently being installed at ATA, but these were not available during the epoch of this work.

[4] In this paper, a 10 minute integration has $N_{observed\_samp} = 4.2e^9 \neq N_{analysis\_chan} = 7e^6$.

are shown in column 5 of Table 1 for reference only. When comparing sensitivities of different detectors, column 4 is the relevant column for an arbitrary MFB irrespective of the actual transmitted signal bandwidth.

The sixth column shows the detection sensitivity of the AC, ACP and PSP detectors used here. The most relevant comparison for these thresholds are column 4. We return to this comparison in the discussion section.

This paper focuses on alternatives to the narrow band search for ETI. In the next section we describe those alternatives and predict their relative sensitivities.

2.3 Three Alternative Detectors

We introduce the new detectors with expressions for their digital computations as compared with that for the traditional power spectrum. For the given observation time the number N_s of digitized samples are broken into N_b equal blocks of length M. Each block is processed to give a detection statistic, which is then averaged over all blocks:

$$\mathrm{PS}(f) = \sum_{n=0}^{N_b-1} \left| \sum_{m=0}^{M-1} \exp\left(-i\,2\pi f\, t_m\right) s(nT + t_m) \right|^2 \tag{2}$$

$$\mathrm{PSP}(f) = \sum_{n=0}^{N_b-1} \left| \sum_{m=0}^{M-1} \exp\left(-i\,2\pi f\, t_m\right) \left| s(mT + t_m) \right|^2 \right|^2 \tag{3}$$

$$\mathrm{AC}(\tau) = \sum_{n=0}^{N_b-1} \left| \sum_{l=0}^{M-1} \frac{\exp\left(i\,2\pi f_l\, \tau\right)}{2\pi} \left| \sum_{m=0}^{M-1} \exp\left(-i\,2\pi f_l\, t_m\right) s(mT + t_m) \right|^2 \right|^2 \tag{4}$$

$$\mathrm{ACP}(\tau) = \sum_{n=0}^{N_b-1} \left| \sum_{l=0}^{M-1} \frac{\exp\left(i\,2\pi f_l\, \tau\right)}{2\pi} \sum_{m=0}^{M-1} \exp\left(-i\,2\pi f_l\, t_m\right) \left| s(mT + t_m) \right|^2 \right|^2 \tag{5}$$

In Eqs. (2)-(5), $s(t_m)$ is the value of sample at point m in the n^{th} block, t_m is the time associated with s measured from the start of the n^{th} block, f_l is the baseband frequency and τ is the time delay measured from the start of the n^{th} block. These equations define the power spectrum (PS), power spectrum of signal power (PSP), autocorrelation (AC), and autocorrelation of power detectors, in that order. As shown, the AC algorithms are implemented using the convolution theorem (Wozencraft & Jacobs, 1990 p. 73) with forward and inverse Fourier transforms.

PS is the ordinary narrowband filter bank. PSP is another MFB where the prototype signal is a potentially wide bandwidth signal whose power is modulated by a sine wave. Note that signals detected with PSP are not necessarily detectable with PS, which was our motivation for monitoring this detection statistic.

AC and ACP are detectors sensitive to regularly repetitive signals (AC) and signals whose power is modulated with a repeating pattern (ACP). Using AC, signals with phase modulation, frequency modulation or amplitude modulation are detectable. ACP is sensitive to amplitude modulated signals. A comparison of AC and ACP is a good first step to understanding the repetitive nature of a signal.

For all detectors, a simple threshold is applied to each signal statistic to identify signals that are very likely to be artificial. To model the statistical behavior, we suppose a continuous signal with power s per time sample. The most probable values of the statistics used for thresholding are:

$$\text{PS} \rightarrow \sqrt{N_b} M\, s^2 \tag{6}$$

$$\text{AC, ACP, PSP} \rightarrow \sqrt{N_b} M \frac{s^4}{(2s+1)^2}. \tag{7}$$

We have chosen units where the mean square value of the noise is 1. Detection is done by visual inspection of graphs of each statistic. As a function of frequency, the threshold values for detection in present study are given in Table 1 with PS in column 4, PSP, AC, or ACP all equal in column 6. Column 6 assumes that the repetition period in terms of samples $N_{rep} \ll N_{chan}$. Each of these numbers should be multiplied by the correction factor $\left(1 - N_{rep} / N_{chan}\right)$ which is different for every signal. In this study, the minimum value for this factor is 0.75, and it was neglected in the analysis.

The convolution algorithm for AC and ACP is important in this application as it costs only 2x more computation than a single variable MFB for narrowband signals (Harp, G. R. et al. 2010a). A more sensitive AC-based algorithm, symbol-wise autocorrelation (Morrison, I. S. 2011a, 2011b) might be pursued in future studies but will require >400,000 times more computation time than for the campaign presented here.

2.4 Observational Design

The ATA is a dual-polarization 42-element interferometer located in Northern California, comprising 6.1 m dishes, dual-linear polarization feeds that operate in 4 simultaneous frequency bands centered anywhere between 1-10 GHz thanks to a patented feed antenna design (Welch, J. et al. 2009).

The signals from ≥ 25 ATA antennas are delayed and summed in a beam former (Barott, W. C. et al. 2011). Complex valued (8-bit real 8-bit imaginary) samples from the beam former are collected at a rate of 8.73 GS/s. The phased array beam diameter can be estimated as $0.1° / f$, where f is the observation frequency in GHz. We make continuous observations with typically 10 minutes on each source. Quasars are effectively point sources for the ATA and many are >100 times more powerful than the background level in a 1 second integration.

Data collections were taken over approximately 14 months in 2010 and 2011. All the source data are freely available on the internet (Harp, G. R. et al. 2010b). Many source targets (69) were chosen because they are known to have fluxes > 1 Jy. We shall see that if the entirety of that flux were repetitively modulated, then it would appear in this survey. Additionally sources for examination were chosen as follows: 1) Exoplanets and Kepler objects of interest (59). Observations of 13 pulsars and the galactic anti-center were performed based on the hypothesis that ET might broadcast in direction opposed to pulsars in their field of view as an aid for our detection of them. Two strong methanol masers were observed using frequency ranges that include their masing frequency (6668 MHz) to see if those masers might be artificially modulated. Six O type stars were chosen to study the hypothesis that advanced extraterrestrials might set up beacons using bright stars as an energy source. Other special pointings include the sun and moon for artifact tests, the Earth-Sun Lagrange L4 point (where artifacts might be left in a stable orbit), the north pole, and one observation toward the same direction[5] of the OSU telescope when the WOW signal appeared (Gray, R. H. & Marvel, K. B. 2001).

Observational frequency bands were selected to be free of strong radio frequency interference (RFI) and often encompass certain "magic" frequencies such as the $\mathrm{H_I}$ line (1.420 GHz), $\sqrt{2}\mathrm{H_I}$ (2.008 GHz), $2\mathrm{H_I}$ (2.840 GHz), $\pi\mathrm{H_I}$ (4.462 GHz), the methanol maser line (6.667 GHz) and 8.4 GHz because it is close to the upper limit of ATA's receivers.

The sampled data from each observation were reduced using Gnu Octave (Eaton, J. W. et al. 1997) to compute the various statistics. The statistics for PSP, AC, and ACP algorithms were computed and plotted followed by visual inspection for peaks or anomalies. Plots of PS were also generated for reference, but not included in the analysis since those types of signals are better detected by the ATA's real time narrowband detector system called SonATA, short for SETI on ATA.

For both AC and ACP, $M = 2^{23}$ or approximately 1 second long. Only positive delays were examined since the spectra are symmetric about zero delay. Inspection was performed over the delay range $1\times10^{-4} < \tau < 0.24$ s, where the lower value is chosen to completely exclude the finite-sized zero delay feature. The time spacing between plotted delays is the same as for the original sampling $\Delta\tau = 1\times10^{-7}$ s.

Interesting signals were noted and if those signals appeared in spectra from more than one pointing, they were identified as a ground or space-based man-made source. Observations were carried out one day per week over approximately 1 year.

3 Results

We demonstrate the utility of AC the detection described here with a few examples of signals we might never have been aware of without those detectors. The strongest and

[5] There are two locations where the WoW! signal might have come from, we chose the location of the "positive" feed at 19.417 hours and -27.05 degrees in right ascention and declination, respectively.

most striking new signals were found with the AC detector, as shown in Figure 3. Here a single observation centered at 1410 MHz is processed for its power spectrum (left) and autocorrelation (right). The PS spectrum shows no evidence of an artificial signal with ~1% random fluctuations about the mean. Meanwhile the AC spectrum displays a sequence of peaks with delays at integer multiples of 1.267 ms that are >100 standard deviations above the mean. The first peak is detected at 200 σ of the mean AC statistic, and we deduce its power to be ~14 Jy.

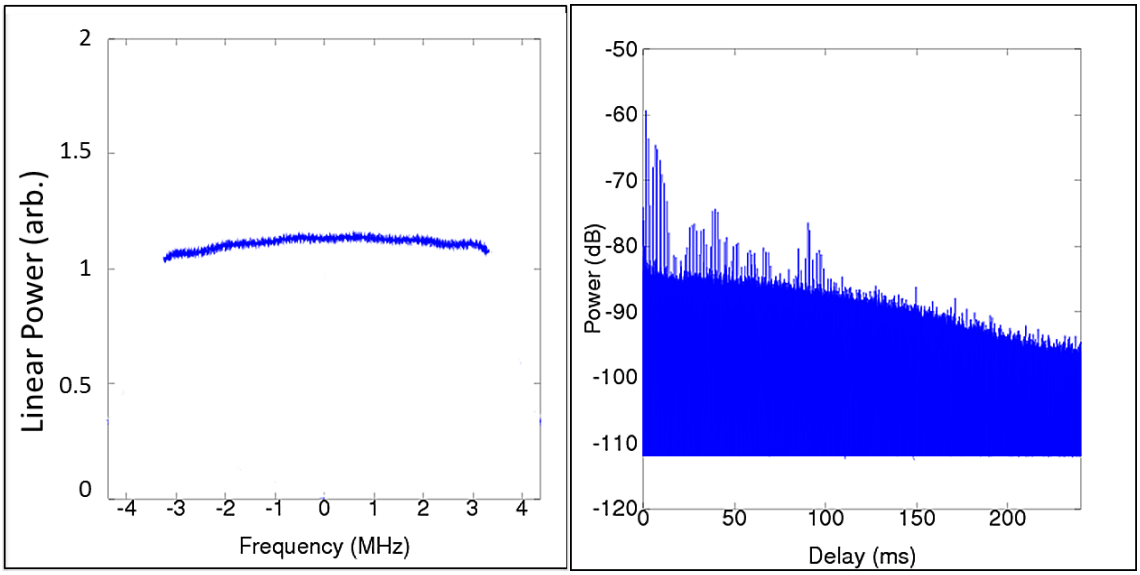

Figure 3: Comparison of PS (left) and AC (right) signal detection applied to a 10-minute data set acquired on the blazar 0714+716 at 1410 MHz.

The signal in Figure 3 is not visible in the PSP or ACP spectra (not shown). The latter indicates that this signal has no amplitude modulation, and probably is phase modulated. This signal was observed over a range of frequencies from 1400-1470 MHz but not much lower or higher than this. This shows how it is not necessary to capture the full bandwidth of an AC signal in order to detect its presence.

We tested for the coherence time of the AC signal by computing the spectrum using different sample block lengths M but keeping all of the data. The first AC peak had a maximum for block time 140 ms, while higher or lower values of M resulted in a smaller peak. This indicates that the repetition period is drifting slowly during the observation, changing by about 1 part in 10^7 in 140 ms.

The signal was observed in various directions, which indicates it must be generated locally and not an ETI signal. The signal may have come from a transmitter on Earth's surface or in geostationary orbit. Despite its strong power, it had never before been identified, though many years of astronomical imaging and SETI surveys at the ATA. How could such a dominating signal be missed? Partly because the signal does not resolve into a narrow feature in the frequency spectrum or in an image. In retrospect, previous imaging work has observed unexpected non-imaging power in correlator output

in the vicinity of the H I line at 1421 MHz, and we tentatively identify the latter with the signal described here.

We note that another interesting signal with repeat period 1.331 ms was also found in multiple pointings in the vicinity of 1420 MHz, with wide bandwidth flux of ~2.5 Jy. It was clearly distinct from the signal of Figure 3 in that its features were 10 times wider and only two features appeared.

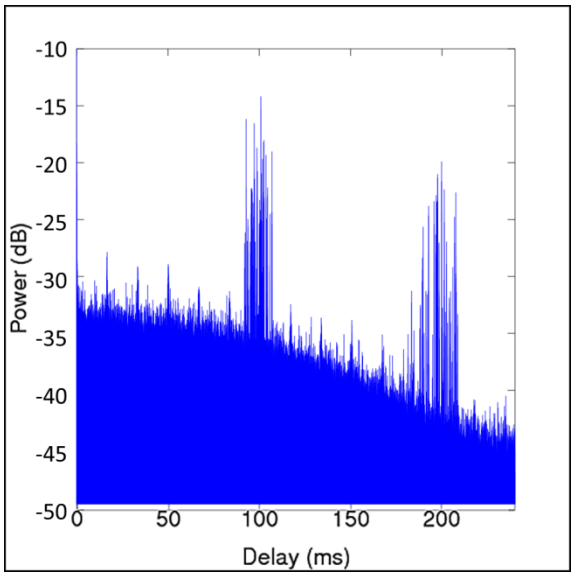

Figure 4: ACP spectrum while pointed toward 3C84 with center frequency 2008 MHz.

Our second example displays an ACP spectrum taken at center frequency 2008 MHz. The narrow structures at multiples of 16.67 ms come from line voltage which shows up at delays for 120 Hz due to the squaring of the signal prior to detection. Such features show up in most ACP spectra and their power spectrum counterparts often appear in PSP spectra (not shown).

The broad, 30 σ features (2.3 Jy) near 100 and 200 ms delay in Figure 4 are of unknown origin, though they appear to be generated on Earth (appear when pointed toward multiple sources). There are no evident counterparts to these features in any other of the detection spectra. These broad features are made up of many small spikes, suggesting that the signal repeats over a short time with one delay value and then switches discontinuously to another, varying over a range of delay values.

We tested the hypothesis that the first and second delay features are similar by comparing the 100 ms feature to a ½ horizontally scaled version of its counterpart at 200 ms (not shown). The distribution of spikes is substantially different for the two features with no visible evidence of similarity. This suggests that the signal modulation is not simply repetitive, but is further modulated in both symbol amplitude as well as symbol length.

Summarizing all the observational results: We found 10 unique signals in PSP, AC and ACP that had no counterparts in PS. All signals were observed multiple times and in

different pointing directions, indicating they arise from terrestrial/satellite communications. None such were observed with center frequency 4462 MHz or above. Happily, this indicates very little RFI over the entire upper half of the terrestrial microwave window (~1-10 GHz), frequencies where new radio SETI observations will be least impacted.

These examples demonstrate a couple of points: 1) AC and ACP are demonstrated to detect repetitive signals that will not be found in a conventional SETI search, and 2) AC and ACP are good detectors for local RFI that may be difficult to characterize otherwise. We do not know of another radio observatory that uses AC as a means of identifying RFI and we suggest that this approach may be useful elsewhere.

4 Discussion

4.1 Archetypal Signal Motivating This Work

This campaign attempts to find signals containing at least some repetitive structure. The archetypal signal here is the wireless Ethernet protocol. Ethernet uses a binary alphabet of symbols to represent arbitrary information, though any finite alphabet can be substituted and our arguments would not change. At the hardware level, each symbol is represented by a particular electromagnetic waveform in the radio frequency band. These symbols are transmitted into space and, intentionally or not, some fraction of those signals escape to great distances from the Earth.

A distant astronomer with a radio telescope and sufficient sensitivity can detect the transmitted data stream in a total power measurement. Because of the pseudo-random nature of symbol order, the astronomer sees broadband power arriving from the direction of Earth. Since many natural sources can generate broadband power, the artificial nature of the signal may be overlooked. Alternatively, if the signal occupies a frequency band not used by the astronomer, then she will not know of its existence.

On the other hand, if the astronomer chooses the right frequency and has sufficient sensitivity to distinguish the waveforms of different signals, then she can employ an AC detector to generate evidence that the signal is indeed artificial.

The AC detectors offer a good way to determine whether or not signals are repetitively modulated. They are well suited to identify signals using the Ethernet protocol and a host of alternative protocols that transmit information using a finite alphabet of symbols. We note that it would be difficult but not impossible to design a symbolic protocol that evades AC detection. Also, almost all modes of human communication are fundamentally symbolic.

4.2 Major Conclusions of Campaign

This is a prototype survey and we have learned much about how to effectively mount an expanded and more sensitive SETI campaign for detection of repetitive signals, as

discussed below. Now we consider the research question[6], "What is the highest probability for the existence of true repetitive ETI signals that is compatible with our results?" We emphasize that since this is the first substantial survey looking for constant-power repetitive signals, we have little *a priori* knowledge to answer this question.

For truly repetitive signals, showing multiple AC or ACP peaks with regular spacing, visual inspection had a sensitivity of $\simeq 1\sigma$ (0.9-1.5 Jy), since multi-peak signals are easy to spot. For signals with shorter coherence length or only a single delay peak, the sensitivity threshold is $\sim 3\sigma$. Using a threshold of 1 Jy for discussion, we consider all sources where the "natural" radiation was equal or greater than this value. A total of 89 independent observations (no repeats of same source and same frequency) were acquired and are listed in the Appendix.

4.2.1 Hypothesis 1

Most previously discovered strong radio sources with flux >1 Jy are modulated with a repeating pattern either directly by extraterrestrials or due to some heretofore unknown physics.

The total population of possible independent observations of sufficiently strong sources can be estimated as follows. The NVSS survey contains 2206 sources with flux ≥ 1 Jy and declination > -40°, corrected to 2690 for the whole sky. The frequency search window, (1-10 GHz) can be divided into 1286 independent 7 MHz ranges. The number of observations required to perform a complete survey with no overlaps is therefore 3.5×10^{6}.

We have 89 independent observations on 23 strong sources, or have performed 2.0×10^{-5} of the complete survey. Assuming a uniform distribution of sources bearing repetitive modulation with probability p_+ of positive detection on any trial, what value of p_+ is consistent with our 89 consecutive observations are negative? We write

$$P = (1-p_+)^{89} < \left(2960*1286\right)^{-1}. \qquad (8)$$

This and other probability results are presented in Table 2. We conclude that $p_+ < 0.16$ for this case. That is, a large majority of potential observations on 1 Jy sources will show negative results. Comparatively, a future search with 1500 observations could attain $p_+ < 0.01$.

Taking a different approach, we assume that if any >1 Jy source is modulated, then it is modulated over its entire transmission band. Following this, our observations on 31 distinct sources leads to the conclusion that no more than 0.22*2690 = 600 are actually modulated.

[6] A more expansive description of our research hypotheses is given in the Introduction.

We reiterate this result including all details: Of the ~2690 radio sources in the sky with flux > 1 Jy in the radio frequency range, no more than 22% of them might bear (either natural or intentional) repetitive modulation with repeat periods between $1\times10^{-4} < \tau < 0.24$.

We conclude that our Hypothesis 1 is untrue.

4.2.2 Hypothesis 2

Most bright pulsars, besides their characteristic repetitive nature, are additionally modulated as above.

According to the ATNF pulsar survey (Manchester, R. et al. 2005) there are 21 pulsars whose integrated flux (at 1400 MHz) is > 1 Jy for a total of 27000 hypothetical observations. This survey made 7 (out of 20 total) independent observations (with negative result) on such pulsars, implying that less than 29% of those pulsars may bear modulation.

We conclude that Hypothesis 2 is untrue.

4.2.3 Hypothesis 3

Most confirmed or "candidate" exoplanets harbor civilizations that transmit powerful messages using radio frequency beams of modulated electromagnetic radiation.

In this section, we make no simplifying assumptions about transmission frequency, and instead work with the product of the number of exoplanet bearing stars with the number of potentially observable bands or star*bands.

The exoplanets considered here orbit stars that have undetectable radio flux for modulation. Hence all the detectable power must come from an artificial transmitter. The current catalog of confirmed or candidate exoplanets includes about 5000 entries including 1667 distinct stars. For 1286 possible frequency band that may be observed, we conclude that no more than 21% exoplanet stars will be found to be actually transmitting in some band.

This excludes Hypothesis 3; instead, most exoplanets are *not* transmitting in a way that they would be seen in our campaign.

4.2.4 Hypothesis 4

Out of all the stars in the galaxy, most harbor transmitters, as in 3.

We made 88 independent observations centered on stars. We conclude that no more than 31% of all stars are transmitting (as defined for this paper) in any band.

This excludes Hypothesis 4.

Table 2:

Source Type	Num Independent Observations	Num Sources in Galaxy	p_+
Distinct Source > 1 Jy	31	2690	0.22
Distinct Pulsar	9	21	0.29
Source Type	Num Independent Observations	Num Star*bands	p_+
(> 1 Jy source)*bands	89	3.46 e+6	0.16
Exoplanet * bands	62	2143762	0.21
Star * bands	88	1.29 e+18	0.31

Other results worthy of comment: The L4 Lagrange point showed no evidence for an artifact transmitting repetitive signals in 3 observations at 1420, 2008 and 3991 MHz.

4.2.5 6668 MHz Methanol Masers

Some naturally occurring astronomical sources can be modulated using beams of energy from external sources. Tommy Gold was the first to suggest that this could be done with an astronomical maser, and just such a maser has been found, (Weisberg, J. M. et al. 2005)), albeit the source of modulation was another natural source (pulsar).

We tested two 6668 MHz methanol masers for evidence of repetitive modulation. Commonly known as W3OH and W51, they emit into ~20 kHz wide bands with peak fluxes of 3471 and 850 Jy respectively. Either of these would appear in our survey if they were modulated. There are only 22 such masers in the galaxy. While we cannot draw decisive conclusions from this sample, we can at least say that the strongest methanol maser known is not repetitively modulated.

4.3 Number of Signal Waveforms Probed

MFB detectors can be created for any basis set of signals with known structure. The number of samples M in one block of the observation is equal to the number of orthogonal signals of one basis or "type" in the filter bank. For example, a single type in a narrowband detector is the set of starting frequencies for given values of the "orthogonal" frequency drift and drift acceleration parameters.

In principle, one wishes to create MFB detectors for a very wide range of signal types including narrowband, pulsed, chirped, and all types of repetitive signals as a start. For repetitive signals, a matched filter offers greater sensitivity to repetitive signals than an AC detector at the cost of a separate many-parameter MFB for each repetition period. In practice MFBs falls far short of this ideal, with usually only narrowband or pulse implementations with only one or two orthogonal variables (e.g. Doppler drift, Doppler acceleration, over a severely limited range compared to what nature permits).

In theory, with three parameters the total number of distinct waveforms probed is $M\,N_s^2$ if all parameters are Nyquist sampled over the full range. For such a MFB, the computation time generally scales as the total number of orthogonal parameter values N_s^2

multiplied by the time to compute a single basis set. In this specific case the computation scales as $\left[M \log_2(M)\right] N_s^2$. This is a small number compared to the number of signal types probed by AC.

Classic and recent theoretical studies of the interstellar medium as a communication channel (Messerschmitt, D. G. & Morrison, I. S. 2012; Drake, F. D. 1965; Shostak, G. S. 1995; Messerschmitt, D. G. 2012) suggest algorithms capable of discovering radio signals that contain information, a good example being AC detection (Harp, G. R. et al. 2010a; Drake, F. D. 1965; Jones, H. W. 1995). Here we describe the first observational radio campaign that employs AC and ACP detectors. Those used here are naturally sensitive to many more signal basis sets than equivalent matched filter detectors for a given computation time.

Autocorrelation is sensitive to signals having *arbitrary* content provided some part of the signal repeats with duration $2 \le n_{rep} \le \frac{M}{2}$ where n_{rep} is the repeat period in samples (up to half the observation length; n_{rep} need not be an integer). Consider the example of binary phase shift symbol encoding and at least 2 symbols per block. The total number of signal waveforms probed by AC in a single analysis is of order $\left(2^{\frac{M}{2}} + 2^{\frac{M-1}{2}} + 2^{\frac{M-2}{2}} ... + 2 \right)$ and dramatically outnumbers those probed by the MFB.

The observations described here have a quadrature sampling rate of 8.73 MCS/s (million complex samples per second), and a block size of $M = 2^{23}$ complex samples or ~1 second duration. Extending the above example, just for binary encodings and one possible repeated message length $\frac{M}{4}$, this analysis will discover any of $2^{2^{21}} \simeq 10^{630000}$ different possible wide-bandwidth waveforms. This is compared to $MN_s^2 \simeq 10^{23}$ for the fully sampled 3 dimensional MFB. Including all possible repeat lengths and all possible symbol encodings, AC probes a practically infinite number of signal types with only twice the computational requirements of a one dimensional matched filter search.

As discussed above this impressive advantage of AC SETI is offset by the fact that a stronger transmitter power is required to excite an AC detector as compared with a MFB. We discuss the interplay of variables in the next section.

We shall conclude that AC searches are best when the source flux exceeds the telescope and sky noise over the integration time. For this reason, we pay special attention to the strongest radio sources in the sky. Radio quasars are exceedingly bright with emission over a continuum of frequencies spanning the frequency range of the ATA (1-10 GHz).

4.4 Figure of Merit

If a source is known to have sufficient flux to trip an AC detector if that flux were modulated, then a matched filter has no advantage over AC except that it searches a small but independent region of signal space.

If the telescope is pointed in a direction with no significant known flux, then the extra sensitivity of a matched filter balances, to some extent, the limited signal space. Far from the transmitter, an electromagnetic signal decreases in areal power density as $1/R^2$, where R is the radius from the transmitter. For a given a transmitter power, the radial reach of a signal is proportional to $1/s^2$, where s is the energy accumulated at the receiver in a single sample. Out to ~1000 LY the number of stars in a sphere radius R goes as R^3 (stellar density of 4.04×10^{-3} ly^{-3}), so the number of stars probed $N_{Stars} \propto P_t^{3/2}$.

For this campaign, the detection threshold energy in one time sample of a sinusoidal signal detected by an analogous MFB is 0.008 Jy s as compared to 0.9 Jy s for AC. The ratio of the number of stars probed by the matched filter to the number probed by AC is therefore $(0.9/0.008)^{3/2} = 1200$. Thus the figure of merit $N_{\text{Stars}}N_{\text{Types}}$ still dramatically favors AC searches over matched filter searches.

A different figure of merit for a SETI search would have to attach essentially zero weight to the number of signal types probed in order to favor the matched filter. For example, it is argued that circularly polarized sinusoid will propagate unperturbed over large interstellar distances. As described above, AC possesses a similar feature, linear perturbations of wide bandwidth signals do not impact detectability.

It may be true that somehow, the spectral transformation (Fourier transform) is more fundamental as tool for signal analysis than other transformations since signals occupying one bin in the frequency spectrum are constant energy or stationary states of the light. If ETI shares this viewpoint, then narrowband signals might be preferred by them, also.

It is hard to quantify how the relative probability for different signal types is affected by this seemingly greater simplicity of the Fourier transform. On the other hand, it has been argued (Messerschmitt, D. G. 2012) that sinusoidal signals are less resistant to RFI and multipath (time variable scintillation induced) fading than spread spectrum, as exemplified by the fact that most Earth-based radio communications are rapidly converging on spread spectrum (wide bandwidth) signals.

4.5 Comparison to KLT

We believe that in the future, most MFB and AC searches will be overtaken by a signal detector based on principle component (a.k.a. eigenvector) decomposition and detection of received signals. In SETI signal processing literature, principle component decomposition is referred to as the Karhunen–Loève Transform (KLT), which renders the received signal into an ordered expansion of orthogonal principle components or eigenvectors where the each component in the expansion carries a power less than or equal to the previous.

While the implementation for signal analysis may vary, the promise of KLT is that an arbitrary (artificial) signal waveform in the presence of Gaussian noise can be optimally detected – with a sensitivity close to that of a MFB. One promising implementation of KLT for SETI is the so-called BAM-KLT (Maccone, C. 2010). For illustration we consider a simplified version of this algorithm.

Assuming an observation with N_s samples representing Gaussian noise plus an arbitrary signal from an ET transmitter. To be picked up by BAM-KLT, this signal must have repetitive structure with repeat length l_{rep} samples (not necessarily an integer). Since we do not know the value of l_{rep}, it is necessary to create a detector with parameter M samples corresponding to the "test" value of l_{rep}.

The algorithm proceeds with breaking the observation up into N_b blocks of samples with length M. These blocks form the rows of a $N_b \times M$ matrix. Because the eigenvectors are ordered by eigenvalue (power content in expansion of signal), only the first few (length M) eigenvectors of this matrix need be computed requiring $O(M^2)$ operations. If M is sufficiently close to l_{rep}, then the eigenvector with the largest eigenvalue is a good approximation of the signal waveform. In a blind search, it is necessary to repeat this process for all values $2 \le M \le M_{\max}$ so the complete calculation scales as $O(M_{\max}^3)$.

By comparison AC detection on the same signal requires $O\left(M_{\max} \ln\left(M_{\max}\right)\right)$ operations. In a more complete calculation for the campaign presented here, BAM-KLT would require approximately 10^{11} times more processing. Despite this computational barrier, we are confident that some KLT variant will eventually prevail in SETI searches since it is optimal for the problem and computationally very highly parallelizable.

4.6 AC for RFI Detection

Radio frequency interference or RFI is an increasingly important problem for radio astronomers and limits the fidelity[7] of ATA synthetic images to one part in 10^{-3}-10^{-4} depending on observation conditions, especially near the hydrogen line at 1420 MHz. We report the detection of a new, strong interferer at the ATA in Figure 3. One reason that this signal was never detected before is that its repeat time of 1.267 ms is longer than the widest inverse bandwidth of our correlator. That is, the narrowest bandwidth setting of the correlator has 6.5 kHz bin size, with an inverse bandwidth of 0.15 ms. Below we will describe how FX[8] correlators can be used to detect signals by AC in future campaigns.

[7] For a given observation O of the flux and the true flux T at a given point, fidelity is defined as $\max(O-T)/T$ and can be estimated with sufficient knowledge of the telescope and the observation conditions.

[8] Described below.

Future telescopes like the square kilometer array aim to achieve greater image fidelity on the order of 10^{-6}. Clearly this cannot be achieved with interferers with fluxes of 10's of Janskys that do not resolve to points in images. We have shown that very strong interferers with repetitive content can remain undetected unless specifically sought for using an AC technique. We recommend that current and future observatories can benefit from monitoring RFI with AC detectors to blank out affected data or to excise the RFI from the images.

4.7 An Improved AC Search Design for the Future

We have shown that AC and ACP detectors probe an immense region of discovery space that is ignored in conventional SETI campaigns. In designing the next generation search we consider two target types: 1) Search for repetition in radiation from known strong sources, and 2) Search for repetitive signals from directions where no strong flux is expected.

Targets having known flux should be chosen such that they carry sufficient flux to trigger AC detection. Here the minimum detectable flux is ~1 Jy. This threshold can be lowered by going to a larger telescope or by increasing the observation time. In fact, the Very Large Array archives contain measurements on all the brightest sources above -20 degrees declination. If the raw correlator data are available, a substantial search for repetitive signals from many more bright sources is possible, down to a sensitivity of ~0.05 Jy, following simple scaling arguments and assuming 10 minutes integration time.

For targets not showing up in previous radio surveys we infer they do not show substantial flux over very wide bandwidths (~10 GHz), but they may show flux over modest bandwidths (Hz to 10's of MHz) not previously detected. An examination of Table 1 shows that such sources would be more easily discovered using a total power imaging survey than with direct application of AC processing. This is because the sensitivity to raw power is greater than the sensitivity to AC.

From these considerations, we propose the next generation SETI detection system should include 3 components. 1) A total power imaging survey covering all frequencies between 1-10 GHz. 2) The equivalent of a 3 parameter MFB that detects chirp traces similar to those in Figure 1 but including all possible slopes and curvatures supported by the data. 3) An autocorrelation detector running in parallel and even using the same data streams as for 1) and 2).

4.8 Direct Computation of AC from Correlator Output

We point out, for the first time, that repetitive SETI signals can be detected in radio interferometer data both in real time and in archives from telescopes such as the ATA, VLA, Westerbork SRT, GMRT, MeerKat, and ASCAP at centimeter wavelengths; LOFAR and other low frequency arrays; and at high frequencies with ALMA. A rich research program could undertake this new style of SETI analysis on archival data with only modest resources. Here we describe the search method and provide a demonstration.

We have mentioned using the output of an FX correlator to detect repetitive signals and here we describe how. Many modern radio interferometers now employ FX imaging

correlators. Here F stands for a Fourier transform, or more accurately a polyphase MFB, performed on finite sequences of samples from each antenna/polarization that together approximate a measure of the electric field in a plane perpendicular to the look direction. The F stage is followed by the X (cross) stage, where spectra from individual antenna/polarizations are multiplied in pairs for a total of $N_{Ant}(N_{Ant}-1)/2$ cross-multiplied spectra, known as spectral visibilities. For large numbers of antennas (>25 or so), the FX algorithm is highly efficient compared with other algorithms such as XF which performs operations in opposite order.

Each spectral visibility is an independent measure of the power spectrum of the correlated signal arriving at two dishes, with processing similar to that in Eq. (2). Thus, the inverse Fourier transform of each spectral visibility is an estimate of the two-point time-correlation function (delay spectrum), exhibiting peaks at all repetition periods. If the image phase center is on the modulated source, then the complex-valued sum of all delay spectra gives the greatest sensitivity. To search for repetitive signals anywhere in the field of view, one can apply a phase-agnostic "averaging" method such as bispectral analysis (Law, C. J. & Bower, G. C. 2012) with only a minor degradation of signal to noise, or even by averaging the amplitudes of delay spectra.

This approach is demonstrated using archival data from a joint experiment between the ATA and the Arecibo Observatory in Figure 5. The Arecibo planetary radar was pointed toward the center of the Moon, and transmissions using binary phase-shift keying (BPSK) were sent with a transmitter bandwidth of 27 MHz. The chip (bit) duration was 0.5μs and the same string of 63 symbols was sent over and over. The signal had no amplitude modulation (only phase) with a repetition rate of 31.5 μs.

The ATA was pointed to the same region on the Moon. The synthetic beam of the ATA is nearly the same diameter as that of Arecibo, so most of the illuminated region of the Moon was in the ATA beam. Arecibo transmitted at 2380 MHz with 250 kW of power. Assuming that this power was 100%[9] diffusely scattered into a hemisphere, and taking into account the distance between Earth and Moon, the proportion arriving in the ATA phased array beam was less than 10^{-4} of the transmitted signal. The ATA filling factor is less than 1%, so the signal entering our array aperture was about 2.5 W; it was so strong that it was difficult to attenuate the signal enough to prevent overdriving the telescope.

Because the radar is circularly polarized, choosing different polarizations on antenna pairs (XY or YX, cross-polarization) captures the reflected signal (shown) just as well as using co-polarization (XX, YY) spectra (not shown for brevity). Visibility spectra from the Moon-bounce observation were Fourier transformed to the delay domain and then summed vectorially. Clear peaks are seen in Figure 5, with delays corresponding to the 31.5 μs repeat time of the transmitted BPSK signal.

[9] This is an over-estimate, since some of the signal is absorbed.

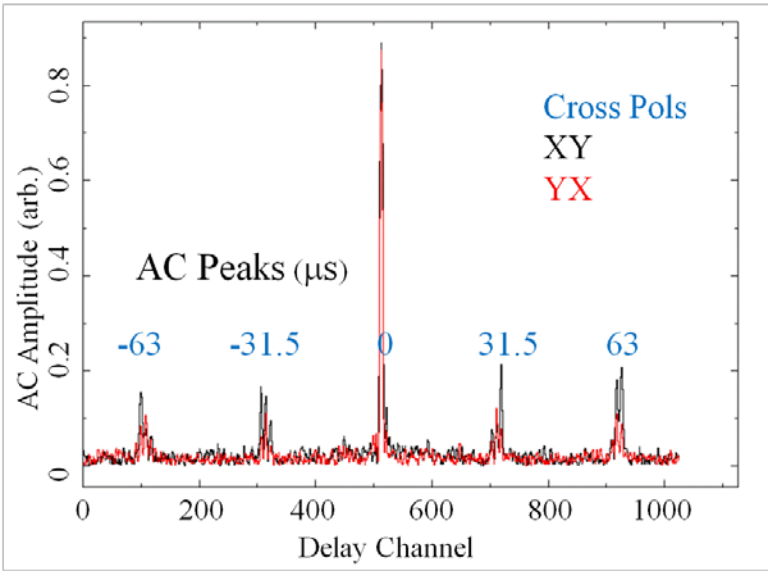

Figure 5: Demonstration of the AC technique using an imaging correlator as detector. Since most modern interferometer telescopes use correlators, this method has wide application.

Compared to the 1,750,000 delay values examined in this survey, AC observations with a correlator are generally more limited in delay range. The ATA correlator has a fixed number of 1024 spectral bins independent of the spectral bandwidth. Thus, no more than 512 delay values may be considered. Since correlators generally integrate over periods measured in seconds (possibly ms periods in the next generation), we are limited to a maximum delay equal to half the inverse bin width. At the ATA, the maximum delay values for 104 MHz to 6.5 MHz settings are 4.8 μs to 77 μs, respectively. Hence AC signal searches are optimized when using the maximum number of channels in the correlator, and different delay ranges can be covered with different correlator observation bandwidths.

4.9 Beyond Detection of AC Signals

Once a repetitive source has been detected as in Figure 5, it is then possible to image the source and determine its position by setting to zero all values in the delay spectrum except those in the vicinity of a peak with finite delay, Fourier transforming once again to the frequency domain, and imaging as usual.

The relationship between artificial repetition and real sky structure deserves further comment. When a point source is within the field of view (FOV), it generally appears as regular oscillations or fringes within the visibility bandwidth for every antenna pair.[10] The fringe period versus frequency depends on the orientation and distance between the antenna pair (baseline), and it is stationary on all baselines when the interferometer is phased up on the source. We call these *structure fringes* because they originate from source structure field of view.

[10] For discussion, assume the source bandwidth is greater than observation bandwidth.

Repetitive sources introduce what we call *delay fringes* into the visibility spectra. Unless mitigated, delay fringes generate spurious structure in the radio image. Unlike structure fringes, delay fringes have the same oscillation period versus frequency in every visibility, independent of the antenna positions. The latter property allows us to distinguish real spatial structure from signal repetition.

Structure fringes show peaks in the delay domain, one for each point source in the image. Sources at phase center peak at zero delay. Sources far from phase center exhibit peaks with a range of positive or negative delays on different baselines. Hence in an image of a region near the phase center, summation over baselines washes out structure peaks from sources outside the field of view.

In comparison, if a repetitive signal (from anywhere) is present, then delay spectrum peaks will appear at the same delay values for all baselines. Because delay fringes transform to a range of differently scaled structure in images, artificial repetitive signals may generate telescope-specific and time-dependent "halos" around the phase center.

Summing delay fringes over baselines reinforces repetition delay peaks relative to structural delay peaks, at once providing a robust detection scheme for identifying artificial repetitive signals. If these signals are unwanted, their interference peaks may be zeroed out in delay spectra after which a Fourier transform back to the frequency domain will result in improved imaging.

5 Conclusions

This paper reports a novel survey of galactic and extra-galactic targets (quasars, supernova remnants, masers, pulsars, stars with known planets, O-type stars, the Lagrange L4 point, etc.) searching for presumably technological signals bearing repetitive structure. Signal detection was performed using ~10 minute observations with 7 MHz effective bandwidth captured to disk at post-processed using 4 methods, two of which use autocorrelation of either the complex-valued stored signal or its power.

The scientific outcomes are laid out in the discussion section and in Table **2**, including:

1. There are 2206 known sources with continuum flux > 1 Jy at 1400 MHz. With an *a priori* confidence level of 99%, we predict any future observation of these sources (excluding duplicates) using the same techniques as used might successfully discover a modulated signal with probability < 0.00015. This is a reduction by a factor of 6600 compared to the *a priori* probability estimate (unity). Taking a step further and assuming that any modulated source is modulated at all frequencies, our results limit the number of such sources to be no more than 1 in the entire galaxy.
2. A similar analysis of pulsar data accumulated from the directions of one of the 21 pulsars with continuum flux > 1 Jy at 1400 MHz indicates that no more than 1/600 of similar observations might be successful. Making the assumption of modulation at all frequencies, we predict only a 3% probability that any one of those 21 pulsars is modulated.

3. There are 22 methanol 6668 MHz masers in the galaxy that are strong enough to be analyzed by the same methods. Multiple observations of two masers were obtained. Here the result is more straightforward since there is only one practical observation frequency and we predict only a 10% chance that one of these masers is repetitively modulated.
4. 105 observations of stars with exoplanets, O-stars, the Earth-Sun L4 Lagrange point, etc. showed no evidence of powerful ETI signals detectable by this survey. It is predicted that similar observations on such sources will detect a modulated signal with probability smaller than 1.3×10^{-4} in each observation.

When a new probe for extraterrestrial signals is introduced, even a modest survey can add greatly to the human reservoir of knowledge. This paper reports the first search for repetitive extraterrestrial signals, some of which might be hiding "in plain sight" but not detected in ordinary analyses of radio telescope data. This principle is demonstrated by the discovery of heretofore unknown and strong repetitive RFI at the ATA. We recommend that other radio observatories should monitor for RFI using autocorrelation techniques to point out interference they may not be aware of.

Finally, we lay the groundwork for a proposed campaign to look for repetitive signals using both real time and archived correlator data, especially on known sources with sufficient flux to trip an AC detector, if that flux were modulated. Without the time consuming and storage consuming requirements of the survey here, AC data come almost for free using existing radio interferometers.

6 Bibliography

Cocconi & Morrison. 1959, *Nature*, 184, 844–846

Drake. 1961, *Phys. Today*, 40

Oliver & Billingham. 1971,

Tarter. 2001, *Annu. Rev. Astron. Astrophys.*, 39, 511–548

Shuch. Springer, 2011,

Harp, Ackermann, Blair, et al. in (Vakoch, D. A.) SUNY Press, 2010a, *Commun. with Extraterr. Intell.*, 45–70

Morrison. 2011a, *Acta Astronaut.*, 78, 90–98

Siemion, Von Korff, McMahon, et al. 2010, *Acta Astronaut.*, 67, 1342–1349

Messerschmitt & Morrison. 2012, *Acta Astronaut.*, 78, 80–89

Harp, Shostak, Tarter, et al. 2012, *Proc. IEEE*, 100, 1700–1717

Von Korff, Demorest, Heien, et al. 2013, *Ap. J.*, 767, 40

Gardner & Spooner. 1992, *IEEE Trans. Commun.*, 40, 149–159

Korpela, Werthimer, Anderson, Cobb & Lebofsky. 2001, *Comput. Sci. Eng.*, 3, 78–83

Tarter, Agrawal, Ackermann, et al. 2010, *SPIE Opt. Eng. Appl.*, 7819, 781902–781902

Wayth, Brisken, Deller, et al. 2011, *Astrophys. J.*, 735, 97

Morrison. 2012, *Acta Astronaut.*, 78, 90–98

Leshem, van der Veen, Boonstra, van der Veen & Boonstra. 2000, *Astrophys. J. Suppl. Ser.*, 131, 355–373

Morrison. 2011b, *ATA Memo Ser.*, 93, 1–31

Weisberg, Johnston, Koribalski & Stanimirovic. 2005, *Science*, 309, 106–10

Harp, Ackermann, Nadler, et al. 2011, *IEEE Antennas Propopagation*, 59, 2004–2021

Wozencraft & Jacobs. Waveland Press, Inc., 1990,

Welch, Backer, Blitz, et al. 2009, *Proc. IEEE*, 97, 1438 – 1447

Barott, Milgrome, Wright, et al. 2011, *Radio Sci.*, 46, RS1016

Harp, Ackermnn, Olsen & Bhatt. 2010b, *SetiQuest Wiki*,

Gray & Marvel. 2001, *Ap. J.*, 546, 1171–1177

Eaton, Bateman & Hauberg. Free Software Foundation, 1997,

Manchester, Hobbs, Teoh & Hobbs. 2005, *Ap. J.*, 129, 1993–2006

Drake. in 1965, *Curr. Asp. Exobiol.*, 323–345

Shostak. in (Shostak, G. S.) 1995, *Prog. Search Extraterr. Life, A.S.P. Conf. Ser. 74*, 447–456

Messerschmitt. 2012, *Acta Astronaut.*, 81, 227–238

Jones. in (Shostak, G. S.) 1995, *Prog. Search Extraterr. Life, V. 74*,

Maccone. 2010, *Acta Astronaut.*, 67, 1427–1439

Law & Bower. 2012, *Ap. J.*, 749, 143

6.1 Appendix: Observation Table

List of all observations collected for this project. The raw data for these observations are available online (Harp, G. R. et al. 2010b). Sources with "off" in their name track the path of the stated object but following the real source with a delay of ~ 1 hr.

Table 3:

List of Observations for This Study

Source	Coordinate	Type	Freq (MHz)	Flux (Jy) @obs freq	Date
0136+478	01 36 59 +47 51 29	quasar	2008	1.7	2010-12-24
0136+478	01 36 59 +47 51 29	quasar	4462	1.9	2010-12-17
0136+478	01 36 59 +47 51 29	quasar	6670	1.9	2010-12-12
0228+673	02 28 50 +67 21 03	quasar	2008	1.2	2011-01-07
0228+673	02 28 50 +67 21 03	quasar	6670	2.0	2010-12-12
0744-064	07 44 22 -06 29 36	quasar	2840	4.7	2010-07-02
0834+555	08 34 55 +55 34 21	quasar	2840	6.8	2010-07-02
0834+555	08 34 55 +55 34 21	quasar	2840	6.8	2010-12-24
0834+555	08 34 55 +55 34 21	quasar	3100	6.6	2010-07-22
0834+555	08 34 55 +55 34 21	quasar	6670	4.4	2010-12-17
1347+122	13 47 33 +12 17 24	quasar	2008	4.6	2010-12-24
1347+122	13 47 33 +12 17 24	quasar	4462	3.0	2010-12-24
1347+122	13 47 33 +12 17 24	quasar	6670	2.7	2010-12-12
1733-130	17 33 03 -13 04 50	quasar	2008	5.1	2011-02-04
1733-130	17 33 03 -13 04 50	quasar	4462	4.8	2010-12-17
1733-130	17 33 03 -13 04 50	quasar	6670	10.1	2010-12-12
2038+513	20 38 37 +51 19 13	quasar	2008	4.9	2011-02-04
2038+513	20 38 37 +51 19 13	quasar	6670	3.4	2010-12-17
2206-185	22 06 10 -18 35 39	quasar	2008	5.8	2011-02-04
2206-185	22 06 10 -18 35 39	quasar	4462	3.9	2010-12-17
3c119	04 32 37 +41 38 28	quasar	2008	7.1	2011-02-04
3c119	04 32 37 +41 38 28	quasar	2840	5.4	2010-07-02
3c119	04 32 37 +41 38 28	quasar	4462	3.9	2010-06-25
3c123	04 37 04 +29 40 14	quasar	2008	39.7	2011-02-04
3c123	04 37 04 +29 40 14	quasar	2840	31.7	2010-07-02
3c123	04 37 04 +29 40 14	quasar	4465	23.6	2010-06-25
3c138	05 21 10 +16 38 22	quasar	2008	7.1	2011-02-04
3c138	05 21 10 +16 38 22	quasar	2840	5.4	2010-07-02
3c138	05 21 10 +16 38 22	quasar	4462	4.0	2010-06-25
3c147	05 42 36 +49 51 07	quasar	2008	18.1	2011-02-04
3c147	05 42 36 +49 51 07	quasar	2840	12.5	2010-07-02
3c147	05 42 36 +49 51 07	quasar	4462	8.6	2010-06-25
3c274	12 30 49 +12 23 29	quasar	2008	3.0	2010-12-24

3c274	12 30 49 +12 23 29	quasar	2840	3.0	2010-07-02
3c274	12 30 49 +12 23 29	quasar	4462	3.0	2010-12-24
3c274	12 30 49 +12 23 29	quasar	6670	3.0	2010-12-17
3c279	12 56 11 -05 47 22	quasar	6670	13.6	2010-12-17
3c286	13 31 08 +30 30 33	quasar	1420	14.9	2010-10-15
3c286	13 31 08 +30 30 33	quasar	2008	12.9	2011-01-07
3c286	13 31 08 +30 30 33	quasar	2008	12.9	2010-12-24
3c286	13 31 08 +30 30 33	quasar	4020	8.4	2010-10-08
3c286	13 31 08 +30 30 33	quasar	6670	6.3	2010-12-12
3c295	14 11 21 +52 12 09	quasar	2008	17.0	2011-01-07
3c295	14 11 21 +52 12 09	quasar	6670	3.0	2010-12-12
3c345	16 42 59 +39 48 37	quasar	2008	7.9	2011-01-07
3c345	16 42 59 +39 48 37	quasar	2008	7.9	2011-02-04
3c345	16 42 59 +39 48 37	quasar	6670	5.5	2010-12-12
3c380	18 29 32 +48 44 46	quasar	2008	10.6	2011-02-04
3c380	18 29 32 +48 44 46	quasar	6670	4.0	2010-12-17
3c395	19 02 56 +31 59 42	quasar	6670	1.2	2010-12-17
3c48	01 37 41 +33 09 35	quasar	1422	16.5	2010-08-13
3c48	01 37 41 +33 09 35	quasar	2008	13.0	2010-12-24
3c48	01 37 41 +33 09 35	quasar	2840	8.9	2010-07-02
3c48	01 37 41 +33 09 35	quasar	4462	5.9	2010-12-17
3c48	01 37 41 +33 09 35	quasar	6670	4.2	2010-12-24
3c84	03 19 48 +41 30 42	quasar	2840	23.6	2010-07-02
3c84	03 19 48 +41 30 42	quasar	4462	23.4	2010-06-25
3c84	03 19 48 +41 30 42	quasar	4462	23.4	2010-09-10
3c84	03 19 48 +41 30 42	quasar	6670	22.1	2010-12-17
Blazars					
BLLacterus	22 02 43 +42 16 40	blazar	1420	6.1	2010-10-15
BLLacterus	22 02 43 +42 16 40	blazar	2008	5.9	2010-10-15
BLLacterus	22 02 43 +42 16 40	blazar	6670	4.2	2010-05-21
BLLacterus	22 02 43 +42 16 40	blazar	8200	4.0	2010-08-13
S5 0716+714	07 21 53 +71 20 36	blazar	1414	~1.5 varies	2010-10-15
S5 0716+714	07 21 53 +71 20 36	blazar	1420	~1.5 varies	2010-10-15
S5 0716+714	07 21 53 +71 20 36	blazar	1420	~1.5 varies	2010-05-21
S5 0716+714	07 21 53 +71 20 36	blazar	1422	~1.5 varies	2010-08-13
S5 0716+714	07 21 53 +71 20 36	blazar	1422	~1.5 varies	2010-08-13
S5 0716+714	07 21 53 +71 20 36	blazar	1422	~1.5 varies	2010-10-15
S5 0716+714	07 21 53 +71 20 36	blazar	1426	~1.5 varies	2010-08-13
S5 0716+714	07 21 53 +71 20 36	blazar	1427	~1.5 varies	2010-10-15
S5 0716+714	07 21 53 +71 20 36	blazar	1432	~1.5 varies	2010-08-13
S5 0716+714	07 21 53 +71 20 36	blazar	1435	~1.5 varies	2010-05-21
S5 0716+714	07 21 53 +71 20 36	blazar	1459	~1.5 varies	2010-10-22
S5 0716+714	07 21 53 +71 20 36	blazar	3086	~1.5 varies	2010-12-17
S5 0716+714	07 21 53 +71 20 36	blazar	6670	~1.5 varies	2010-10-22
S5 0716+714	07 21 53 +71 20 36	blazar	8200	~1.5 varies	2010-05-07

0954+658	09 58 47 +65 33 55	blazar	1432	~1.3 varies	2010-10-15
0954+658	09 58 47 +65 33 55	blazar	8200	~1.3 varies	2010-10-22
Supernova Remnants and Masers					
taua	05 34 32 +22 00 58	SNR	2008	1110.0	2010-08-13
taua	05 34 32 +22 00 58	SNR	1420	1110.0	2010-05-07
taua	05 34 32 +22 00 58	SNR	2840	1110.0	2010-10-15
casa	23 23 27 +58 48 28	SNR	2008	1547.3	2010-08-13
casa	23 23 27 +58 48 28	SNR	4462	885.9	2010-10-15
casa	23 23 27 +58 48 28	SNR	6670	701.1	2010-08-13
w51	19 23 44 +14 30 33	maser	6670	850 peak	2010-05-07
w3oh	02 27 04 +61 52 25	maser	6670	3741 peak	2010-03-26
w3oh	02 27 04 +61 52 25	maser	6670	3741 peak	2010-04-02
w3oh	02 27 04 +61 52 25	maser	6670	3741 peak	2010-05-07
Pulsars				@1400 MHz	
crab	05 34 32 +22 00 52	pulsar	2008	12.6	2011-02-04
crab	05 34 32 +22 00 52	pulsar	1420	12.6	2010-03-26
crab	05 34 32 +22 00 52	pulsar	1420	12.6	2010-10-15
crab	05 34 32 +22 00 52	pulsar	2600	12.6	2010-03-09
crab	05 34 32 +22 00 52	pulsar	4462	12.6	2010-05-07
crab	05 34 32 +22 00 52	pulsar	1420	12.6	2010-05-07
crab	05 34 32 +22 00 52	pulsar	4462	12.6	2010-06-25
psrb0329+54	03 32 59 +54 34 44	pulsar	1420	1.8	2010-05-07
psrb0329+54	03 32 59 +54 34 44	pulsar	1420	1.8	2010-05-21
psrb0329+54	03 32 59 +54 34 44	pulsar	611	1.8	2011-03-04
psrb0450+55	04 54 08 +55 43 42	pulsar	4462	0.3	2010-06-25
psrb0809+74	08 14 59 +74 29 06	pulsar	4462	0.0	2010-06-25
psrb0809+74	08 14 59 +74 29 06	pulsar	1420	0.0	2010-05-14
psrb0823+26	08 26 51 +26 37 24	pulsar	4462	0.1	2010-06-18
psrb0823+26	08 26 51 +26 37 24	pulsar	4462	0.1	2010-06-25
psrb0950+08	09 53 09 +07 55 36	pulsar	4462	3.2	2010-06-18
psrb0950+08	09 53 09 +07 55 36	pulsar	4462	3.2	2010-06-25
psrb1133+16	11 36 03 +15 51 04	pulsar	4462	0.9	2010-06-25
psrb1237+25	12 39 40 +24 53 49	pulsar	4462	0.4	2010-06-25
psrb1937+21	19 39 39 +21 34 59	pulsar	1420	0.3	2010-11-05
Stars - Including Kepler Exoplanets, O-stars					
koi001	13 12 44 -31 52 24	exoplanet	4462	<1	2010-09-10
koi044	22 53 13 -14 15 13	exoplanet	4462	<1	2010-03-26
koi051	09 34 50 -12 07 46	exoplanet	4462	<1	2010-09-10
koi054	10 58 28 -10 46 13	exoplanet	4462	<1	2010-09-10
koi060	03 32 55 -09 27 29	exoplanet	1420	<1	2010-03-19
koi062	12 44 20 -08 40 17	exoplanet	4462	<1	2010-09-10
koi071	11 35 52 -04 45 21	exoplanet	4462	<1	2010-09-10
koi072	22 09 40 -04 38 27	exoplanet	4462	<1	2010-03-26
koi073	09 56 06 -03 48 30	exoplanet	4462	<1	2010-09-10

koi076	12 19 13 -03 19 11	exoplanet	4462	<1	2010-09-10
koi080	13 12 43 -02 15 54	exoplanet	4462	<1	2010-09-10
koi081	10 42 48 -02 11 01	exoplanet	4462	<1	2010-09-10
koi084	11 24 17 -01 31 44	exoplanet	4462	<1	2010-09-10
koi096	11 45 42 +02 49 17	exoplanet	4462	<1	2010-09-10
koi097	11 26 46 +03 00 22	exoplanet	4462	<1	2010-09-10
koi112	12 13 29 +10 02 29	exoplanet	4462	<1	2010-09-10
koi117	10 18 21 +12 37 15	exoplanet	4462	<1	2010-09-10
koi118	13 28 26 +13 47 12	exoplanet	4462	<1	2010-09-10
koi119	11 46 24 +14 07 26	exoplanet	4462	<1	2010-09-10
koi125	13 12 19 +17 31 01	exoplanet	4462	<1	2010-09-10
koi126	10 10 07 +18 11 12	exoplanet	4462	<1	2010-09-10
koi127	23 18 47 +18 38 45	exoplanet	3100	<1	2010-07-22
koi130	04 42 56 +18 57 29	exoplanet	1420	<1	2010-03-19
koi133	09 23 47 +20 21 52	exoplanet	3100	<1	2010-07-22
koi134	00 44 41 +20 26 56	exoplanet	4462	<1	2010-03-26
koi144	00 39 21 +21 15 01	exoplanet	1420	<1	2010-03-19
koi150	02 04 34 +25 24 51	exoplanet	4462	<1	2010-03-26
koi155	11 42 11 +26 42 23	exoplanet	4462	<1	2010-09-10
koi160	08 52 37 +28 20 02	exoplanet	1420	<1	2010-03-19
koi172	00 20 40 +31 59 24	exoplanet	4462	<1	2010-03-26
koi191	22 57 47 +38 40 30	exoplanet	3100	<1	2010-07-22
koi195	10 59 29 +40 25 46	exoplanet	4462	<1	2010-09-10
koi201	10 22 10 +41 13 46	exoplanet	4462	<1	2010-09-10
koi201	10 22 10 +41 13 46	exoplanet	3100	<1	2010-07-22
koi202	01 36 48 +41 24 38	exoplanet	1420	<1	2010-03-19
koi208	06 04 29 +44 15 37	exoplanet	3100	<1	2010-07-22
koi211	19 28 59 +47 58 10	exoplanet	1420	<1	2010-09-24
koi211	19 28 59 +47 58 10	exoplanet	4462	<1	2010-10-01
koi216	07 48 07 +50 13 33	exoplanet	3100	<1	2010-07-22
koi219	14 56 55 +53 22 56	exoplanet	1420	<1	2010-09-24
koi219	14 56 55 +53 22 56	exoplanet	4462	<1	2010-10-01
koi220	13 34 02 +53 43 42	exoplanet	4462	<1	2010-09-10
koi221	15 35 16 +53 55 20	exoplanet	1420	<1	2010-09-24
koi221	15 35 16 +53 55 20	exoplanet	4462	<1	2010-10-01
koi222	18 10 32 +54 17 12	exoplanet	4462	<1	2010-10-01
koi225	07 21 33 +58 16 05	exoplanet	4462	<1	2010-10-01
koi226	15 24 55 +58 57 57	exoplanet	4462	<1	2010-10-01
koi227	08 18 22 +61 27 38	exoplanet	4462	<1	2010-10-01
koi228	08 40 13 +64 19 41	exoplanet	4462	<1	2010-10-01
koi231	12 05 15 +76 54 20	exoplanet	4462	<1	2010-09-10
koi233	05 22 33 +79 13 52	exoplanet	3100	<1	2010-07-22
koi236	13 00 03 +12 00 07	exoplanet	4462	<1	2010-09-10
Gliese581	15 19 27 -07 43 20	exoplanet	1420	<1	2010-10-01
Gliese581	15 19 27 -07 43 20	exoplanet	4462	<1	2011-01-28

Gliese581	15 19 27 -07 43 20	exoplanet	4462	<1	2010-10-01
koi04	19 02 28 +50 08 09	exoplanet	1418	<1	2010-05-14
koi04	19 02 28 +50 08 09	exoplanet	1420	<1	2010-01-22
koi04	19 02 28 +50 08 09	exoplanet	1420	<1	2010-03-19
koi04	19 02 28 +50 08 09	exoplanet	1420	<1	2010-03-19
koi04	19 02 28 +50 08 09	exoplanet	1420	<1	2010-04-02
koi04	19 02 28 +50 08 09	exoplanet	1420	<1	2010-09-24
koi04	19 02 28 +50 08 09	exoplanet	1420	<1	2010-11-05
koi04	19 02 28 +50 08 09	exoplanet	1420	<1	2010-05-14
koi04	19 02 28 +50 08 09	exoplanet	1692	<1	2010-09-24
koi139.01	19 26 37 +44 41 18	exoplanet	1690	<1	2011-03-31
koi174.01	19 47 18 +48 06 27	exoplanet	1690	<1	2011-03-31
koi268.01	19 02 55 +38 30 25	exoplanet	1690	<1	2011-03-31
koi51.01	19 43 40 +41 19 57	exoplanet	1690	<1	2011-03-31
koi70.03	19 10 48 +42 20 19	exoplanet	1690	<1	2011-03-31
55Cancri	08 52 36 +28 19 51	OZMA star	1420	<1	2010-11-05
zetaOph	16 37 10 -10 34 02	O-star	1420	<1	2010-11-05
zetaOph	16 37 10 -10 34 02	O-star	2008	<1	2010-12-24
zetaOph	16 37 10 -10 34 02	O-star	2840	<1	2010-12-24
zetaOph	16 37 10 -10 34 02	O-star	6670	<1	2010-12-17
HD172175	18 39 04 -07 51 35	O-star	1420	<1	2010-11-05
HD166734	18 12 25 -10 43 53	O-star	1420	<1	2010-11-05
HD093521	10 48 24 +37 34 13	O-star	1420	<1	2010-11-05
HD060848	07 37 06 +16 54 15	O-star	1420	<1	2010-11-05
BD114586	18 18 03 -11 17 39	O-star	1420	<1	2010-11-05
Special Pointings					
Sun	N/A	Sun	1414	~1000000	2010-10-15
Sun	N/A	Sun	1420	~1000000	2010-10-15
Sun	N/A	Sun	1426	~1000000	2010-10-15
Moon	N/A	Moon	1420	~10000	2010-10-08
Moon	N/A	Moon	1420	~10000	2010-11-05
northpole	00 00 00 +90 00 00	North Pole	1543	<1	2010-10-22
northpole	00 00 00 +90 00 00	North Pole	3086	<1	2010-10-22
Lagrange-4	Sun-Earth L4	Lagrange point	1420	<1	2010-10-08
Lagrange-4	Sun-Earth L4	Lagrange point	2008	<1	2010-10-08
Lagrange-4	Sun-Earth L4	Lagrange point	3991	<1	2010-10-08
galanticenter	05 45 37 +28 56 10	Galactic Anticenter	1420	<1	2010-05-07
galanticenter	05 45 37 +28 56 10	Galactic Anticenter	1422	<1	2010-05-07
galanticenter	05 45 37 +28 56 10	Galactic Anticenter	3991	<1	2010-05-07

galanticenter	05 45 37 +28 56 10	Galactic Anticenter	3991	<1	2010-10-08
galanticenter	05 45 37 +28 56 10	Galactic Anticenter	4462	<1	2010-05-07
galanticenter	05 45 37 +28 56 10	Galactic Anticenter	2008	<1	2010-05-07
galanticenter	05 45 37 +28 56 10	Galactic Anticenter	3991	<1	2010-10-08
WoW	19 25 31 -26 57 00	Legend	1430	<1	2011-02-18
Confirmation Observations (intentionally away from some particular source)					
blank06	06 00 00 +40 00 00	off beam	1422		?
blank06	06 00 00 +40 00 00	off beam	1427		?
blank18	18 00 00 +70 00 00	off beam	6670		?
blank18	18 00 00 +70 00 00	off beam	2008		?
blank	09 18 06 -11 54 17	off beam	2840		?
off EpsilonEridani	03 32 56 +09 27 30	off beam	1420		?
off EtaAreitis	02 12 48 +21 12 39	off beam	1420		?
off galanticenter	05 45 37 +33 56 10	off beam	2008		?
off galanticenter	05 45 37 +33 56 10	off beam	3991		?
off Gliese581	15 19 27 +07 43 20	off beam	4462		?
off Gliese581	15 19 27 +07 43 20	off beam	1420		?
off HD69830	08 18 24 +12 37 56	off beam	1420		?
off TauCeti	01 44 04 +15 56 15	off beam	1420		?
Confirmation Observations (surveying RFI at ATA)					
AZEL360-18	fixed az, el	sweep	1410		?
AZEL345-18	fixed az, el	sweep	1410		?
AZEL330-18	fixed az, el	sweep	1410		?
AZEL315-18	fixed az, el	sweep	1410		?
AZEL300-18	fixed az, el	sweep	1410		?
AZEL285-18	fixed az, el	sweep	1410		?
AZEL270-18	fixed az, el	sweep	1410		?
AZEL255-18	fixed az, el	sweep	1410		?
AZEL240-18	fixed az, el	sweep	1410		?
AZEL225-18	fixed az, el	sweep	1410		?
AZEL210-18	fixed az, el	sweep	1410		?
AZEL195-18	fixed az, el	sweep	1410		?
AZEL180-18	fixed az, el	sweep	1410		?
AZEL165-18	fixed az, el	sweep	1410		?
AZEL150-18	fixed az, el	sweep	1410		?
AZEL135-18	fixed az, el	sweep	1410		?
AZEL120-18	fixed az, el	sweep	1410		?
AZEL105-18	fixed az, el	sweep	1410		?
AZEL090-18	fixed az, el	sweep	1410		?

AZEL075-18	fixed az, el	sweep	1410	?
AZEL060-18	fixed az, el	sweep	1410	?
AZEL045-18	fixed az, el	sweep	1410	?
AZEL030-18	fixed az, el	sweep	1410	?
AZEL015-18	fixed az, el	sweep	1410	?